Chapter 9
Beamforming in Coupled-Oscillator Arrays

In this chapter, convex optimization and other global optimization techniques are used to demonstrate the beamforming capabilities of coupled-oscillator arrays and to optimize the stability of the coupled-oscillator array steady-state solution. An introduction to convex optimization is presented followed by several optimization problems showing the beamforming capabilities of such arrays, such as pattern-nulling, difference-beam generation, and multiple-beam generation [96,118,150,151,152]. A global optimization algorithm is also presented that permits one to optimize the stability of the steady-state solution, and therefore leads to more robust solutions and maximizes the obtained stable beam-scanning limits [153]. Finally, the operation of a coupled-oscillator array as an adaptive beamforming system is demonstrated [154].

9.1 Preliminary Concepts of Convex Optimization

Convex optimization is a class of optimization problems that has enjoyed an increased scientific interest in the recent years due to the development of very efficient algorithms essentially rendering their solution as easy as the solution of linear programs [133]. As a result convex optimization problems have found wide application in fields such as control and signal processing, and among these, in the problem of antenna array beam-steering and beamforming. Due to this fact, in this chapter we first present a brief introduction to convex optimization and the mathematical framework required to express the beamforming problem as a convex optimization problem and additionally

introduce the coupled-oscillator array solutions presented in the previous chapters as constraints to the problem at hand.

An optimization problem is expressed in the form

$$\begin{aligned} &\text{minimize } f_o(\boldsymbol{x}) \\ &\text{subject to } f_i(\boldsymbol{x}) \le b_i \quad i = 1, \ldots, M \end{aligned} \tag{9.1-1}$$

where $\boldsymbol{x}$ is the optimization variable, a vector of dimension N. The real function f_o is called the objective function of the problem, and real f_i are the M constraints of the problem with limits or bounds b_i [133]. The family of convex optimization problems consists of those optimization problems where both the objective and the constraints satisfy the property of convexity. In convex optimization problems, a local minimum is also a global minimum; and therefore, once a solution is found, it is guaranteed to be optimal. Additionally, there exist many computationally efficient algorithms for solving convex optimization problems, such as the interior point methods [155]. As a result, once an optimization problem is formulated as a convex one, its efficient resolution is guaranteed.

A set C is *convex* if for every two points $\boldsymbol{x}$ and $\boldsymbol{y}$ of dimension N that belong to the set and any real number θ such that $0 \le \theta \le 1$, the point $\boldsymbol{z} = \theta\boldsymbol{x} + (1-\theta)\boldsymbol{y}$ also belongs in C. Geometrically this means that any point z that lies on the line segment connecting $\boldsymbol{x}$ and $\boldsymbol{y}$ must belong to C. If, instead, θ is allowed to take any real value, then the set C is called *affine*. Correspondingly, an affine set contains every point on the line that is defined by two points $\boldsymbol{x}$ and $\boldsymbol{y}$. These concepts are illustrated in Fig. 9-1.

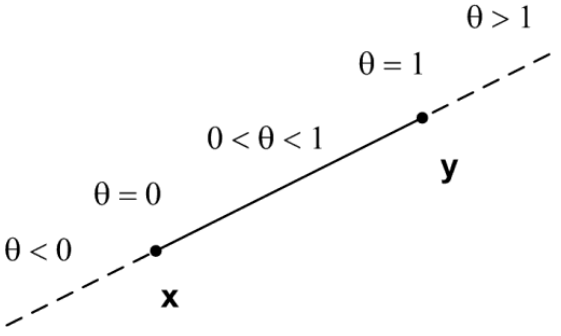

Fig. 9-1. Geometric interpretation of convex and affine sets.

Some well known convex sets are line segments and half spaces [133]. A half-space is the solution set of a linear inequality of the form

$$\{\boldsymbol{x} \,|\, \boldsymbol{a}^T\boldsymbol{x} \leq \boldsymbol{b}\} \tag{9.1-2}$$

where $\boldsymbol{a} \neq \boldsymbol{0}$. The hyperplane defined by the linear equality

$$\{\boldsymbol{x}|\boldsymbol{a}^T\boldsymbol{x} = \boldsymbol{b}\} \tag{9.1-3}$$

is an affine set ($\boldsymbol{a} \neq \boldsymbol{0}$) that separates the space of N dimensional real vectors into two convex half-spaces corresponding to the inequalities $\boldsymbol{a}^T\boldsymbol{x} \leq \boldsymbol{b}$ and $\boldsymbol{a}^T\boldsymbol{x} \geq \boldsymbol{b}$. A hyperplane is defined by a point $\boldsymbol{x_o}$ and a nonzero vector $\boldsymbol{a}$**,** and it contains all vectors $\boldsymbol{x}$ such that the difference vector $\boldsymbol{x} - \boldsymbol{x_o}$ is orthogonal to $\boldsymbol{a}$ (Fig. 9-2)**.**

A norm ball with center $\boldsymbol{x_c}$ and radius r is a convex set defined by

$$\{\boldsymbol{x}|\|\boldsymbol{x} - \boldsymbol{x_c}\| \leq r\} \tag{9.1-4}$$

where $\|\boldsymbol{x}\|$ is a properly defined norm of $\boldsymbol{x}$, such as for example the Euclidean norm. Furthermore, a norm cone is is a convex set defined as the set of $(\boldsymbol{x}, t)$ pairs such that

$$\{(\boldsymbol{x}, t)|\|\boldsymbol{x}\| \leq t\} \tag{9.1-5}$$

If the Euclidean norm $\|\boldsymbol{x}\|_2 = \sqrt{\sum_{i=1}^{N} x_i^2}$ is considered then the corresponding norm cone is called a second-order cone, or ice-cream cone [133].

A real function f_i is convex if its domain is a convex set and if for any two vectors $\boldsymbol{x}$ and $\boldsymbol{y}$ in its domain, the following inequality holds

$$f_i(a\boldsymbol{x} + b\boldsymbol{y}) \leq af_i(\boldsymbol{x}) + bf_i(\boldsymbol{y}) \tag{9.1-6}$$

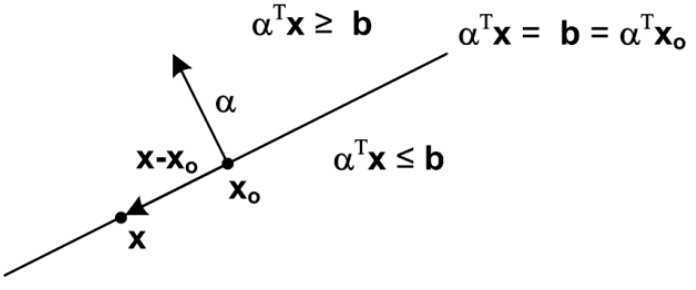

Fig. 9-2. Geometric interpretation of hyperplane and hyperspace.

where a and b are non-negative real numbers such that $a + b = 1$. One can easily verify from Eq. (9.1-6) that a linear function is convex. Another commonly used convex constraint is a linear matrix inequality [156]

$$\boldsymbol{F}(\boldsymbol{x}) = \boldsymbol{F_o} + \sum_{i=1}^{N} x_i \boldsymbol{F_i} > 0 \tag{9.1-7}$$

where $\boldsymbol{x} = [x_n]$ is a vector of dimension N and $\boldsymbol{F_i} = \boldsymbol{F_i^T}$ are real symmetric matrices of dimension M. A real square matrix $\boldsymbol{F}(\boldsymbol{x})$ is positive definite $\boldsymbol{F}(\boldsymbol{x}) > 0$, if for any nonzero vector $\boldsymbol{u}$, $\boldsymbol{u^T F}(\boldsymbol{x})\boldsymbol{u} > 0$. Many convex constraints such as linear inequalities, convex quadratic inequalities, and Lyapunov matrix inequalities can be cast in the form of a linear matrix inequality. According to Lyapunov theory, the system of differential equations

$$\dot{\boldsymbol{x}} = \boldsymbol{A}\boldsymbol{x} \tag{9.1-8}$$

is stable if and only if exists a positive definite matrix $\boldsymbol{P} > \boldsymbol{0}$ such that

$$\boldsymbol{A^T P} + \boldsymbol{P A} < 0 \tag{9.1-9}$$

The above inequality is known as a Lyapunov matrix inequality. The inequality of Eq. (9.1-9) with the matrix $\boldsymbol{P}$ as unknown can be cast in the form of a linear matrix inequality [156].

The minimization of the maximum eigenvalue of a matrix $\boldsymbol{A}$ subject to a linear matrix inequality constraint $\boldsymbol{B}(\boldsymbol{x}) > 0$ is a convex problem defined as [156]

$$\begin{gathered} \text{minimize } \lambda \\ \text{subject to } \lambda \boldsymbol{I_N} - \boldsymbol{A}(\boldsymbol{x}) > \boldsymbol{0}\,, \boldsymbol{B}(\mathbf{x}) > \boldsymbol{0} \end{gathered} \tag{9.1-10}$$

with $\boldsymbol{A}$ and $\boldsymbol{B}$ symmetric matrices that depend affinely on $\boldsymbol{x}$. If one defines an extended unknown vector $\boldsymbol{y} = [\boldsymbol{x} \quad \lambda]^T$ and $\boldsymbol{c} = [\boldsymbol{0_N} \quad 1]^T$ the eigenvalue minimization problem can be written as minimization of a linear function subject to a linear matrix inequality

$$\begin{gathered} \text{minimize } \boldsymbol{c^T y} \\ \text{subject to } \boldsymbol{F}(\boldsymbol{y}) > \boldsymbol{0} \end{gathered} \tag{9.1-11}$$

where $\boldsymbol{B}(\mathbf{x}) > \boldsymbol{0}$ together with $\boldsymbol{\lambda I_N} - \boldsymbol{A}(\boldsymbol{x}) > \boldsymbol{0}$ have been formulated as a single linear matrix inequality $\boldsymbol{F}(\boldsymbol{y}) > \boldsymbol{0}$.

Linear programming and least-squares optimization are two well known examples of convex optimization problems. In linear programming, both the objective and the constraints are linear functions

$$\begin{gathered} \text{minimize } \boldsymbol{c^T x} \\ \text{subject to } \boldsymbol{a_i^T x} \leq \boldsymbol{b_i} \;\; i = 1, \ldots, M \end{gathered} \tag{9.1-12}$$

In least squares optimization the objective function is a sum of squares which is a convex function and there are no constraints

$$\text{minimize } \|\boldsymbol{Ax}-\boldsymbol{b}\|_2^2=\sum_{i=1}^{M}\left(\boldsymbol{a_i^T x}-b_i\right)^2 \tag{9.1-13}$$

Where $\boldsymbol{A}=[a_{mn}]$ is an M by N matrix, $\boldsymbol{a_i}$ is a vector of dimension N containing the elements of column i of matrix **A**, and $\boldsymbol{b}$ is a vector of dimension M.

Finally, the minimization of the maximum generalized eigenvalue of a pair of symmetric matrices $\boldsymbol{A}$ and $\boldsymbol{B}$ that depend affinely on $\boldsymbol{x}$, subject to an additional linear matrix inequality constraint $\boldsymbol{C}(\boldsymbol{x})>0$ is a quasi-convex optimization problem [156] expressed as

$$\begin{gathered}\text{minimize } \lambda \\ \text{subject to } \lambda\boldsymbol{B}(\boldsymbol{x})-\boldsymbol{A}(\boldsymbol{x})>\boldsymbol{0}\,,\boldsymbol{B}(\boldsymbol{x})>\boldsymbol{0}\,,\boldsymbol{C}(\boldsymbol{x})>\boldsymbol{0}\end{gathered} \tag{9.1-14}$$

A real function f is quasi-convex if and only if its domain is a convex set, and for any two vectors $\boldsymbol{x}$ and $\boldsymbol{y}$ in its domain, and a real number θ, such that $0\le\theta\le 1$, the following inequality holds [133]

$$f(\theta\boldsymbol{x}+(1-\theta)\boldsymbol{y})\le\max\{f(\boldsymbol{x}),f(\boldsymbol{y})\} \tag{9.1-15}$$

Convex functions are also quasi-convex but not vice-versa. The standard formulation of a quasi-convex optimization problem has a quasi-convex objective and convex constraints. The generalized eigenvalue minimization problem given by Eq. (9.1-14) can be written in the standard format [156,133]. Similarly to convex optimization problems, quasi-convex optimization problems can also be solved efficiently.

9.2 Beamfoming in COAs

The ability to generate constant phase distributions among the coupled-oscillator array elements by tuning the frequency of only the edge array elements has been one of the most attractive properties of coupled-oscillator arrays as they can be used in beam-scanning applications eliminating the need for phase shifters or a complicated local-oscillator feed network. If, however, one is allowed to tune the frequency of more or all the array elements, then additional features maybe introduced in the radiated pattern such as placement of nulls at desired far-field angular directions.

Once a constant progressive phase shift is established among the array elements, the main beam direction is steered towards a desired direction. In Ref. [157], Steyskal showed that additional nulls maybe formed in the radiation pattern at desired angular directions by introducing small perturbations to the

phases of the array elements. This method was used by Heath [96] in conjunction with the generalized phase model to demonstrate beamforming capabilities using coupled-oscillator arrays. Finally, Georgiadis et al. [118] extended Heath's work by including both amplitude and phase perturbations. In the following, a description of this beamforming methodology is provided.

The array factor of a uniform linear antenna-array of N elements is given by

$$F(\theta) = \sum_{n=1}^{N} V_n e^{j(nkd\sin\theta+\phi_n)} \tag{9.2-1}$$

where the element distance is d, and the angular direction θ is measured from broadside. The main beam is steered at $\theta_o$when the excitation amplitudes are equal $V_n = V_o$ and the element phases are set as $\phi_{on} = -nkd\sin\theta_o$. The array factor is then written in compact form

$$F(\theta) = V_o \boldsymbol{u^H 1_N} \tag{9.2-2}$$

where $\boldsymbol{u}(\theta) = \left[e^{-j(nkd\sin\theta+\phi_{on})}\right]$. If one introduces a perturbation in the excitation amplitudes and phases $\boldsymbol{x} = [\boldsymbol{\Delta V^T} \quad \boldsymbol{\Delta\phi^T}]^{\boldsymbol{T}}$ the array factor is approximated to first order as

$$F(\theta) = V_o \boldsymbol{u^H 1_N} + u^H[\boldsymbol{I_N} \quad jV_o\boldsymbol{I_N}]\boldsymbol{x} \tag{9.2-3}$$

A constraint in the array factor at angle θ_1 is introduced by imposing $|F(\theta_1)| \leq f_1$ where f_1 is a desired maximum level at θ_1. Given $M < N$ level constraints, one may form a complex vector $\boldsymbol{U = C + jS} = [F(\theta_1)\, F(\theta_2) \ldots F(\theta_M)]^T$ containing all the constraints and a second one containing $\boldsymbol{f} = [f_1\, f_2 \ldots f_M]^T$ and combine them in a matrix inequality

$$\begin{bmatrix} -V_o\boldsymbol{C1_N} - \boldsymbol{f} \\ -V_o\boldsymbol{S1_N} \end{bmatrix} \leq \begin{bmatrix} \boldsymbol{C} & -V_o\boldsymbol{S} \\ \boldsymbol{C} & V_o\boldsymbol{C} \end{bmatrix} \boldsymbol{x} \leq \begin{bmatrix} -V_o\boldsymbol{C1_N} + \boldsymbol{f} \\ -V_o\boldsymbol{S1_N} \end{bmatrix} \tag{9.2-4}$$

which can be written in compact form

$$\boldsymbol{f_l \leq Fx \leq f_h} \tag{9.2-5}$$

The beamforming problem can be formulated as a convex optimization problem as follows

$$\begin{aligned} &\min_{\boldsymbol{x}} t \\ &\text{subject to } \|\boldsymbol{x}\| \leq t \\ &\boldsymbol{f_l \leq Fx \leq f_h} \end{aligned} \tag{9.2-6}$$

where the linear objective is subject to a second-order cone constraint and a linear inequality. Minimizing the norm of $\boldsymbol{x}$ ensures that the perturbation approximation of the array factor is valid.

The problem given by Eq. (9.2-6) was analytically solved by Georgiadis et al. in Ref. [118] for the case where the inequality constraints are null constraints ($\boldsymbol{f_l = f_h = 0}$). In fact, the analytical solution to this problem when considering phase perturbations only was given by [157]. In this case [157,118],

$$t_{min} = (\boldsymbol{C1_N})^{\boldsymbol{T}}(\boldsymbol{SS^T})^{-\boldsymbol{T}}(\boldsymbol{C1_N}) \tag{9.2-7}$$

and

$$\Delta\boldsymbol{\phi_{min}} = \boldsymbol{S^T}(\boldsymbol{SS^T})^{-\boldsymbol{1}}(\boldsymbol{C1_N}) \tag{9.2-8}$$

It is interesting to study Eq. (9.2-7), for the simple case of main-beam direction at $\theta_o$with one nulling constraint at angle θ_1. One then evaluates t_{min}as

$$t_{min} = \frac{[\sum_1^N \cos(nkd\alpha)]^2}{\sum_1^N \sin^2(nkd\alpha)} \tag{9.2-9}$$

where $a = \sin\theta_1 - \sin\theta_o$. This shows that there exist combinations of θ_o and $\theta_1$such that the required perturbation magnitude t_{min} goes to infinity, for which the optimization problem does not have a solution. These solutions correspond to $mkda = q\pi$ where m and q are integers. One such solution is for $a = 0$, which corresponds to $\theta_1 = \theta_o$; or in other words, when the desired null is in the direction of the main lobe. A second solution is when

$$\sin\theta_1 - \sin\theta_o = \frac{\pi}{kd} \tag{9.2-10}$$

which corresponds to a desired null direction θ_1 that depends on the main beam angle θ_o. The existence of such points was also verified numerically for the case of a coupled-oscillator array in [118,150].

In order to apply the pattern constraints to the coupled oscillator array, one needs to limit the perturbation vectors $\boldsymbol{x}$ satisfying Eq. (9.2-6) to the set that corresponds to a coupled-oscillator array steady-state solution. Reference [118] introduced the coupled-oscillator array steady-state solution in Eq. (9.2-6) as an additional linear constraint maintaining the convexity of the optimization problem. The steady-state solution (7.7-12)is first reformulated to reflect the nature of perturbation $\boldsymbol{x}$, which contains both amplitude $V_n = V_o + \Delta V_n$ and phase perturbations $\phi_n = \phi_{on} + \Delta\phi_n = -nkd\sin\theta_o + \Delta\phi_n$. Due to the autonomous nature of the coupled oscillator array, the steady-state solution is defined by the relative phases of the oscillator elements. In other words, the phase of one oscillator maybe set to an arbitrary value, or alternatively the phases of all oscillators can be changed by an equal amount without affecting the steady state. This is verified by the steady-state expression Eq. (7.6-10) where only phase differences are present. Consequently, a perturbation of the steady state is set by considering the terms $\Delta\phi_n$ such that even though

individually they may take large values, their relative differences are kept small. This argument was also used in the early works of Kurokawa [105] when modeling the externally injection-locked oscillator. It is, therefore, possible to approximate the phase exponents appearing in Eq. 7.6-10 as

$$e^{j(\phi_n-\phi_m)} \approx e^{j(\phi_{on}-\phi_{om})}[1+j(\Delta\phi_n-\Delta\phi_m)]$$

and obtain the perturbed steady state as

$$\begin{bmatrix}\boldsymbol{C_V I_N}+\boldsymbol{\Phi^H C_c \Phi} & \boldsymbol{C_\phi I_N}\end{bmatrix}\boldsymbol{x}+\boldsymbol{C_\mu \Delta\mu}+j\Delta\omega\mathbf{1}_N+\boldsymbol{\Phi^H C_c \Phi 1_N} = 0 \tag{9.2-11}$$

with

$$\boldsymbol{C_\phi} = \boldsymbol{j}[\boldsymbol{\Phi^H C_c \Phi} - \mathrm{dg}(\boldsymbol{\Phi^H C_c \Phi 1_N})] \tag{9.2-12}$$

The final system of equations is obtained by separating real and imaginary parts

$$\begin{bmatrix}\boldsymbol{C_V^R I_N}+\left(\boldsymbol{\Phi^H C_c \Phi 1_N}\right)^R & \boldsymbol{C_\phi^R I_N} & \boldsymbol{C_\mu^R I_N}\\ \boldsymbol{C_V^I I_N}+\left(\boldsymbol{\Phi^H C_c \Phi 1_N}\right)^I & \boldsymbol{C_\phi^I I_N} & \boldsymbol{C_\mu^I I_N}\end{bmatrix}\begin{bmatrix}\boldsymbol{x}\\ \boldsymbol{\Delta\mu}\end{bmatrix} = -\begin{bmatrix}\left(\boldsymbol{\Phi^H C_c \Phi 1_N}\right)^R\\ \Delta\omega\mathbf{1}_N+\left(\boldsymbol{\Phi^H C_c \Phi 1_N}\right)^I\end{bmatrix} \tag{9.2-13}$$

which is written in compact form

$$[\boldsymbol{G} \quad \boldsymbol{G}_{\Delta\mu}]\begin{bmatrix}\boldsymbol{x}\\ \boldsymbol{\Delta\mu}\end{bmatrix} = \boldsymbol{g} \tag{9.2-14}$$

Using the above linear constraint for the steady state, it is possible to formulate the beamforming optimization problem for coupled oscillator arrays [118] as follows

$$\begin{gathered}\min_{\boldsymbol{x},\boldsymbol{\Delta\mu}} t\\ \text{subject to } \|\boldsymbol{x}\|+\|\boldsymbol{\Delta\mu}\| \le t\\ \boldsymbol{f_l} \le \boldsymbol{F x} \le \boldsymbol{f_h}\\ [\boldsymbol{G} \quad \boldsymbol{G}_{\Delta\mu}]\begin{bmatrix}\boldsymbol{x}\\ \boldsymbol{\Delta\mu}\end{bmatrix} = \boldsymbol{g}\end{gathered} \tag{9.2-15}$$

where the norm of the vector $\boldsymbol{\Delta\mu}$ is also minimized in order to enforce the perturbation condition pertaining to the derivation of the steady-state constraint. The above formulation was extended to planar arrays in Ref. [150].

Once the steady state is obtained, its stability is examined by considering the linear variational system corresponding to the system of differential equations describing the coupled oscillator dynamics and evaluating the eigenvalues of matrix $\boldsymbol{K}$ or $\widetilde{\boldsymbol{K}}$ in Eq. (7.7-17).

We may further explore the arbitrary phase reference of the coupled oscillator array in order to minimize the number of optimization variables in Eq. (9.2-15). $\boldsymbol{G}$ is a square matrix of dimension $2N$. It has one zero eigenvalue due to the fact that the array steady state is unaffected by applying an arbitrary but constant phase term to all elements. It is therefore possible, without loss of generality, to set the phase perturbation of an arbitrarily selected element j to zero $\Delta\phi_j = 0$ and eliminate the column of $\boldsymbol{G}$ that corresponds to $\Delta\phi_j$. Then, a new steady-state vector $\boldsymbol{y} = \left[\boldsymbol{\Delta V}^{\mathbf{T}} \quad \boldsymbol{\Delta\widetilde{\phi}}^{\mathbf{T}} \quad \Delta\mu_j\right]^T$ of dimension $2N$ is constructed, where $\boldsymbol{\Delta\widetilde{\phi}}$ contains all phase perturbations except $\Delta\phi_j$. Using $\boldsymbol{y}$, Eq. (9.2-14) is rearranged in the form

$$\left[\widetilde{\boldsymbol{G}} \quad \boldsymbol{G}_{\Delta\widetilde{\boldsymbol{\mu}}}\right]\begin{bmatrix}\boldsymbol{y}\\ \Delta\widetilde{\boldsymbol{\mu}}\end{bmatrix} = \boldsymbol{g} \Rightarrow \widetilde{\boldsymbol{G}}\boldsymbol{y} = \widetilde{\boldsymbol{g}}(\Delta\widetilde{\boldsymbol{\mu}}) \tag{9.2-16}$$

where $\Delta\mu_j$ is the control perturbation corresponding to the selected element j. $\widetilde{\boldsymbol{G}}$ is a full rank square matrix of dimension $2N$ obtained from $\boldsymbol{G}$ by substituting its column corresponding to $\Delta\phi_j$ with the column of $\boldsymbol{G}_{\Delta\boldsymbol{\mu}}$ corresponding to $\Delta\mu_j$. Similarly $\boldsymbol{G}_{\Delta\widetilde{\boldsymbol{\mu}}}$, has dimension $2N$ by $N-1$ and is obtained from $G_{\Delta\mu}$ by eliminating the column that corresponds to $\Delta\mu_j$. The matrix $\boldsymbol{g}(\Delta\widetilde{\boldsymbol{\mu}})$ is linearly dependent on $\Delta\widetilde{\boldsymbol{\mu}}$. The steady state $\boldsymbol{y}$ is therefore expressed as a function of the $N-1$ independent control variables $\Delta\widetilde{\boldsymbol{\mu}}$. Following Georgiadis et al. [153], the equality constraint of Eq. (9.2-16) is used to eliminate the $2N$ optimization variables included in $\boldsymbol{y}$, and formulate Eq. (9.2-15) in terms of only the independent $N-1$ control variables $\Delta\widetilde{\boldsymbol{\mu}}$

$$\begin{aligned}&\min_{\Delta\widetilde{\boldsymbol{\mu}}} t\\ &\text{subject to } \left\|\widetilde{\boldsymbol{G}}^{-\mathbf{1}}\widetilde{\boldsymbol{g}}(\Delta\widetilde{\boldsymbol{\mu}})\right\| + \|\Delta\widetilde{\boldsymbol{\mu}}\| \le t\\ &\boldsymbol{f}_{\Delta\widetilde{\boldsymbol{\mu}}\boldsymbol{l}} \le \boldsymbol{F}_{\Delta\widetilde{\boldsymbol{\mu}}}\Delta\widetilde{\boldsymbol{\mu}} \le \boldsymbol{f}_{\Delta\widetilde{\boldsymbol{\mu}}\boldsymbol{h}}\end{aligned} \tag{9.2-17}$$

where the equality constraint is now eliminated and the inequality constraints on the array factor have been appropriately reformulated in terms of the independent control variables. As an example, let us consider the five-element coupled oscillator array of Section 8.4, assuming that each oscillator output is connected to an antenna, and the antenna elements are placed a half free-space wavelength apart ($kd = \pi$). The free-running oscillator steady state corresponds to an amplitude of $V_o = 0.442$ V (the output power is 2.9 dBm), and frequency $f_o = 9.892$ GHz obtained for a control voltage of $\mu_o = 10$ V.

The coupling network consists of a transmission line section of 360 deg electrical length at f_o and two series resistors $R = 150\ \Omega$ (Fig. 8-9). The optimization problem given by Eq. (9.2-17) was solved for the case of main beam direction at $\theta_o = 0$ deg (broadside) and an additional null constraint at $\theta_1 = -60$ deg. The outcome of the optimization procedure is shown in Table 9-1. The phase perturbation of the middle array element 3 was arbitrarily set to zero. The steady-state vector y consisted of the five oscillator amplitude perturbations; the four phase perturbations of oscillators 1,2,4, and 5; and the control voltage of the middle oscillator 3. Correspondingly, the optimization variables were the control voltages of elements 1, 2, 4, and 5.

The resulting array factor is shown in Fig. 9-3. In addition to the result of the optimization problem given by Eq. (9.2-17), the array factor corresponding to the solution of problem given by Eq. (9.2-6) (which does not contain the array steady-state constraint) was also included for comparison, as well as the array factor corresponding to uniform excitation without a null constraint. It can be verified that the null is successfully imposed in the array factor at the expense of higher side-lobe levels and a small shift in the main lobe direction. For this particular case, the solutions of Eqs. (9.2-17) and (9.2-6) overlap, which indicates that there exists a steady-state solution for the coupled-oscillator array that satisfies the pattern constraints given by Eq. (9.2-6).

The optimization problem given by Eq. (9.2-17) was then solved for different values of the coupling resistor R, and the solution stability was examined by calculating the eigenvalues of the linear variational system of differential equations corresponding to the array steady state. The critical eigenvalue having the largest real part (spectral abscissa) is shown in Fig. 9-4 for different values of R. It is seen that, as coupling becomes weaker, the solution eventually becomes unstable. The change of stability occurs for a coupling resistor value of 178 Ω .

Table 9-1. Pattern nulling optimization of Eq. (9.2-17) applied in a five-element linear coupled-oscillator array. The main beam direction is $\theta_o = 0$ deg (broadside). A null in the array factor is imposed at $\theta_1 = -60$ deg.

Element	Amplitude ΔV (Volt)	Phase $\Delta\phi$ (°)	Control $\Delta\mu$ (Volt)
1	0.0026	–16.257	–0.093
2	–0.0031	5.292	0.119
3	–0.0001	0	0.004
4	0.0033	–6.178	–0.127
5	–0.0027	16.331	0.097

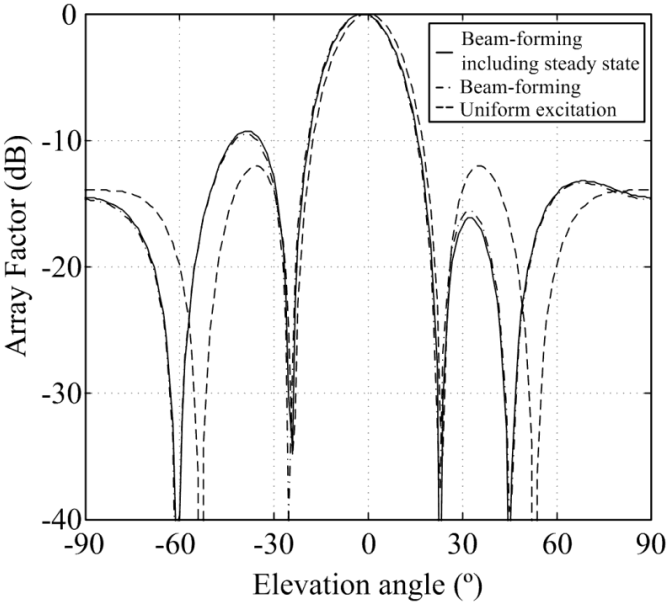

Fig. 9-3. Beamforming capabilities of coupled oscillator arrays. Array factor of five-element array of Section Error! Reference source not found. **for main beam at broadside and one null constraint at $\theta_1 = -60$ deg. The coupling resistor is $R = 150\ \Omega$.**

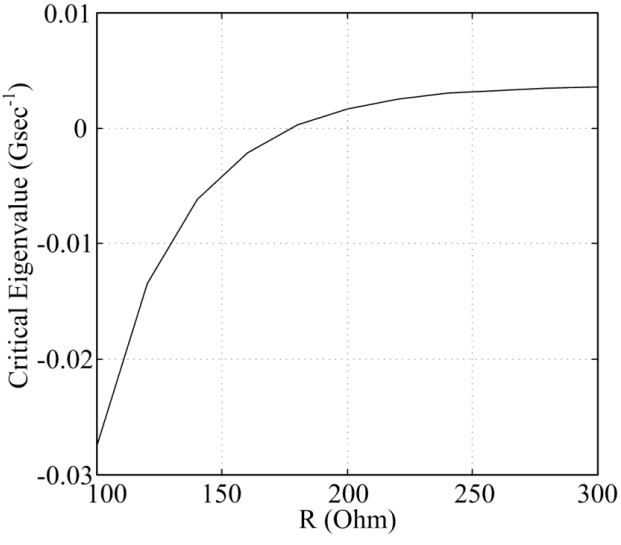

Fig. 9-4. Critical eigenvalue of the solution of the optimization problem of Eq. (9.2-17) versus the coupling resistor R.

9.3 Stability Optimization of the Coupled-Oscillator Steady-State Solution

The stability of the coupled oscillator steady-state solution is verified by examining the linear variational equations corresponding to the system of nonlinear differential equations describing its dynamics. In Section 7.7, a procedure was described to remove the zero eigenvalue that appears due to the free-running nature of the oscillator array. The resulting square matrix $\widetilde{\boldsymbol{K}}$ of dimension $2N-1$ was derived in Section7.7, where N is the size of the array. The linear variational equation for $\boldsymbol{\delta\tilde{x}} = [\boldsymbol{\delta V^T} \quad \boldsymbol{\delta\tilde{\phi}^T}]^{\boldsymbol{T}}$ is repeated here for convenience, where $\boldsymbol{\delta\tilde{\phi}}$ contains $N-1$ phase differences with respect to an arbitrarily selected oscillator j as a reference

$$\boldsymbol{\delta\dot{\tilde{x}}} = \widetilde{\boldsymbol{K}}\boldsymbol{\delta\tilde{x}} \tag{9.3-1}$$

By definition, a steady-state solution is stable if the spectral abscissa of $\widetilde{\boldsymbol{K}}$ is negative. The decay rate of $\widetilde{\boldsymbol{K}}$ is the negative of the spectral abscissa [156], and a steady state is stable if $\widetilde{\boldsymbol{K}}$ has a positive decay rate. Maximizing the decay rate corresponds to a more robust steady-state solution, less likely to lose its stability due to the presence of noise or other perturbations. The matrix $\widetilde{\boldsymbol{K}}(\Delta\boldsymbol{\tilde{\mu}})$ depends on the steady state defined by the perturbation vector $\boldsymbol{x} = [\boldsymbol{\Delta V^T} \quad \boldsymbol{\Delta\phi^T}]^{\boldsymbol{T}}$ of the array, which, following Eq. (9.2-16), is determined by the (perturbation) vector of $N-1$ control voltages $\Delta\boldsymbol{\tilde{\mu}}$. $\widetilde{\boldsymbol{K}}$ does not depend linearly on $\Delta\boldsymbol{\tilde{\mu}}$ due to the matrix inversion involved in its derivation and due to the fact that the phase terms appear in exponential terms. This can be easily verified following the formulation that leads to the definition of $\widetilde{\boldsymbol{K}}$ in Section 7.7. However, due to the fundamental assumption that $\boldsymbol{x}$ and $\Delta\boldsymbol{\tilde{\mu}}$ are small, we may consider the first order expansion $\widetilde{\boldsymbol{K}}_{\boldsymbol{L}}(\Delta\boldsymbol{\tilde{\mu}})$ of $\widetilde{\boldsymbol{K}}(\Delta\boldsymbol{\tilde{\mu}})$. The derivation of $\widetilde{\boldsymbol{K}}_{\boldsymbol{L}}(\Delta\boldsymbol{\tilde{\mu}})$ is straightforward.

A lower bound on the decay rate can be obtained using Lyapunov theory as the maximum q that solves [156]

$$\dot{V}_K(\boldsymbol{\delta x}) < -2qV_K(\boldsymbol{\delta x}) \tag{9.3-2}$$

for any δx, where $V_K(\boldsymbol{x})$ is a scalar quadratic potential function defined by a 0real symmetrix matrix P with dimension $2N-1$ such that

$$V_K(\boldsymbol{\delta x}) = \boldsymbol{\delta x^T P \delta x} \tag{9.3-3}$$

Using Eqs. (9.3-1) and (9.3-3) in Eq. (9.3-2), one obtains a matrix inequality

$$\boldsymbol{P}\widetilde{\boldsymbol{K}}_{\boldsymbol{L}} + \widetilde{\boldsymbol{K}}_{\boldsymbol{L}}^{\boldsymbol{T}}\boldsymbol{P} + 2q\boldsymbol{P} < 0 \tag{9.3-4}$$

For a given steady state $\Delta\tilde{\mu}$, finding the symmetric positive definite matrix $\boldsymbol{P}$ that maximizes the decay rate q is a generalized eigenvalue optimization

problem. Conversely, given a specific matrix $\boldsymbol{P}$ finding the steady state $\Delta\widetilde{\boldsymbol{\mu}}$ that maximizes q is an eigenvalue optimization problem. As noted in Section 9.1, both such problems can be efficiently solved using convex optimization algorithms. However, finding the steady state $\Delta\widetilde{\boldsymbol{\mu}}$ and matrix $\boldsymbol{P}$ that maximize q is not a convex optimization problem due to the multiplicative terms that appear between the elements of $\Delta\widetilde{\boldsymbol{\mu}}$ and $\boldsymbol{P}$.

It is possible to introduce the decay-rate optimization constraint in the coupled-oscillator array beamforming optimization algorithm following the approach by Georgiadis and Slavakis [153], which is given below. The optimization problem including the stability constraint is written as follows

$$\begin{aligned} & L(t,q) = \min_{\Delta\widetilde{\boldsymbol{\mu}},\boldsymbol{P}}(t-q) \\ \text{subject to (i)} \quad & \left\|\widetilde{\boldsymbol{G}}^{-1}\widetilde{\boldsymbol{g}}(\Delta\widetilde{\boldsymbol{\mu}})\right\| + \|\Delta\widetilde{\boldsymbol{\mu}}\| \le t \\ \text{(ii)} \quad & \boldsymbol{F}_{\Delta\widetilde{\boldsymbol{\mu}}}\Delta\widetilde{\boldsymbol{\mu}} \le \boldsymbol{f}_{\Delta\widetilde{\boldsymbol{\mu}}\boldsymbol{h}} \\ \text{(iii)} \quad & \boldsymbol{P}\widetilde{\boldsymbol{K}}_{\boldsymbol{L}}(\Delta\widetilde{\boldsymbol{\mu}}) + \widetilde{\boldsymbol{K}}_{\boldsymbol{L}}^{\boldsymbol{T}}(\Delta\widetilde{\boldsymbol{\mu}})\boldsymbol{P} + 2q\boldsymbol{P} < \boldsymbol{0} \\ \text{(iv)} \quad & \boldsymbol{P} > 0 \end{aligned} \tag{9.3-5}$$

This is not a convex optimization problem, and its resolution is not straightforward. In Ref. [153], an algorithm was proposed to obtain a solution to the above problem by alternative minimization of two sub-problems, an eigenvalue and a generalized eigenvalue problem. The algorithm proceeds as follows

Step 1: Let $e > 0$ be the algorithm termination tolerance and $k = 0$ be the iteration number. Find $\Delta\widetilde{\boldsymbol{\mu}}_{\boldsymbol{k}} = \Delta\widetilde{\boldsymbol{\mu}}_{\boldsymbol{o}}$, the vector of control variables that minimizes the perturbation vector norm $t = t_o$, subject to (i) and (ii). This is the original convex optimization problem of Eqs. (9.2-17) and (9.2-15) that does not include a stability constraint. Obtain the decay rate q_o corresponding to $\widetilde{\boldsymbol{K}}_{\boldsymbol{L}}(\Delta\widetilde{\boldsymbol{\mu}}_{\boldsymbol{o}})$ by evaluating its eigenvalues.

Step 2: Repeat {

P1: Find the real symmetric square matrix $\boldsymbol{P}_{\boldsymbol{k+1}}$ that minimizes $L(0,q) = -q$, subject to (iii) and (iv) for a given $\Delta\widetilde{\boldsymbol{\mu}}_{\boldsymbol{k}}$. This is a generalized eigenvalue optimization problem. The optimization objective provides a value of the decay rate $q_{1,k+1}$.

P2: Find the control vector $\Delta\widetilde{\boldsymbol{\mu}}_{\boldsymbol{k+1}}$ that minimizes $L(t,q) = t - q$ using as input the matrix $\boldsymbol{P}_{\boldsymbol{k+1}}$ obtained from the previous step. This is an eigenvalue optimization problem. Additional outputs of this step are the norm of the perturbation vector t_{k+1} and the decay rate $q_{2,k+1}$.

P3: $k = k + 1$

} until $\left(q_{2,k+1} - q_{1,k+1}\right) < e$

The algorithm is demonstrated for the case of the five-element coupled-oscillator array considered in Section 9.2, where the main beam was directed broadside ($\theta_o = 0$ deg) and a null in the array factor was placed at $\theta_1 = -60$ deg. For a coupling resistor $R = 150\ \Omega$ the beamforming optimization problem in Eq. (9.2-17) obtained the stable solution indicated in Table 9-1. The decay rate of this solution was 3.83 Msec^{-1}, as shown in Fig. 9-4. Using this solution as a starting point the above algorithm was run in order to find a solution of Eq. (9.3-5) with an optimum decay rate. The algorithm converged after 11 iterations using a termination tolerance of 10^{-5}. The result from P1 and P2 for the various steps of the algorithm is plotted in Fig. 9-5. The final solution of the algorithm had a decay rate of 13.2 Msec^{-1} (which is more than three times the initial value).

The perturbation vector of this solution is indicated in Table 9-2, where one can verify that it is only slightly increased from the original solution of Table 9-1 ($t = 0.484$ compared to the original perturbation of $t = 0.480$). Finally, the radiation pattern of the final solution is almost identical to the radiation pattern of the original starting point solution, shown in Fig. 9-3.

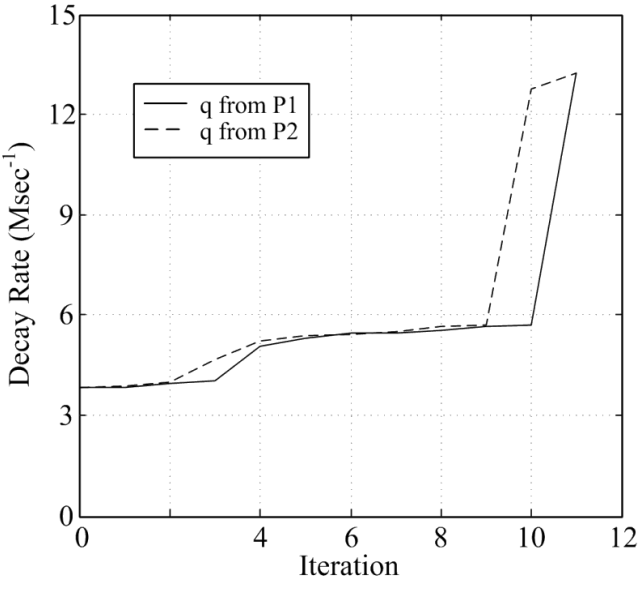

Fig. 9-5. Decay rate of the optimization problem Eq. (9.3-5) versus the iteration number.

Table 9-2. Pattern nulling and stability optimization in Eq. (9.3-5) applied in a five-element linear coupled-oscillator array. The main beam direction is $\theta_o = 0$ deg (broadside). A null in the array factor is imposed at $\theta_1 = -60$ deg.

Element	Amplitude $\Delta \boldsymbol{V}$ (Volt)	Phase $\Delta \boldsymbol{\phi}$ (deg)	Control $\boldsymbol{\Delta \mu}$ (V)
1	0.0025	–17.870	–0.089
2	–0.0027	2.868	0.105
3	–0.0002	0	0.007
4	0.0030	–4.354	–0.114
5	–0.0026	17.033	0.092

9.4 Multi-Beam Pattern Generation Using Coupled-Oscillator Arrays

The synthesis of antenna radiation patterns was formulated as a convex optimization problem by Lebret and Boyd [158]. Considering a uniform linear array for simplicity, its array factor is given by

$$F(\theta) = \sum_{n=1}^{N} v_n e^{jnkd \sin\theta} = \boldsymbol{S}(\theta)^H \boldsymbol{v} \tag{9.4-1}$$

where the vector $\boldsymbol{v} = [v_n] = \left[V_n e^{j\phi_n}\right]$ contains the complex excitations of each element, the element distance is d, and θ is measured from broadside. This formulation is slightly different from the one used in the previous section in order to emphasize the fact that the array factor is a linear function of the complex element excitations.

The pattern-synthesis convex optimization problem is written as [151,158]

$$\begin{gathered} \min_{\boldsymbol{v}} t \\ \text{subject to } |F(\theta_i)| < t \ , \ \forall\, i \ \in 1, \dots, M \\ |F(\theta_k)| < U_k \ , \ \forall\, k \ \in 1, \dots, P \\ \left|F\left(\theta_q\right)\right| = 1 \ , \ \forall\, q \in 1, \dots, L \end{gathered} \tag{9.4-2}$$

The above formulation contains L equality constraints corresponding to L array factor maxima at angular directions θ_q. Moreover, there exist P maximum level U_k constraints and M array factor minimization constraints. As a result, it is possible to efficiently obtain the complex excitations required to synthesize arbitrary patterns, such as ones having multiple beams and other beam-shaping requirements. Furthermore, the number of the optimization variables maybe

minimized by using the equality constraints to solve for and eliminate L-dependent variables [158].

Due to the fact that an arbitrary pattern synthesis problem cannot be considered as a perturbation of some initial reference pattern, such as for example the one corresponding to uniform in-phase excitation, the linear constraint for the coupled oscillator steady state given by Eq. (9.2-14) or (9.2-16) cannot not be used, as the desired steady state may require a large perturbation vector $\boldsymbol{x}$ or $\boldsymbol{y}$, especially in terms of the oscillator phase differences. As a result, the general pattern synthesis problem applied to coupled-oscillator arrays may be approached in three steps. First one obtains the required complex excitations by solving the convex optimization problem Eq. (9.4-2). Second, once the desired amplitude and phase values are found, one uses the steady-state equations corresponding to the coupled-oscillator models in Eq. (7.4-4) or (7.7-12) (which do not assume a linear perturbation for the phase terms) in order to find the coupled-oscillator steady state that closely matches the required amplitude and phase distribution. For example, when using Eq. 7.7-12), one may substitute the phase values obtained by solving Eq. (9.4-2) in the previous step and solve Eq. (7.7-12) for the amplitude and control variables. Alternatively, a nonlinear simulator (such as harmonic-balance optimization) can be used, where the phase values are imposed and fixed, and the amplitude values obtained from convex optimization are used only to initialize the oscillator amplitudes in the simulation and are allowed to be optimized together with the control parameters in order to obtain the steady state. Third, once a coupled-oscillator steady state has been selected, the stability of the solution must be verified, for example by calculating the eigenvalues corresponding to the linear variational system of the array dynamics around the steady state. In fact, as will be seen in the following examples, in this step the designer synthesizes the coupling network in order to guarantee the stability of the steady-state solution.

Difference pattern generation using coupled-oscillator arrays was demonstrated by Heath in Ref. [31]. Heath considered a linear coupled oscillator array, and using the generalized phase model to describe its dynamics, extended the application of the beam-steering model initially introduced by York [111] to difference pattern generation and steering. He showed that a stable difference pattern maybe generated by a simple modification in the coupling network, that is, by introducing a 180-deg phase shift in the coupling between the central elements of the array, while maintaining a 0-deg phase shift between all remaining elements. In order to steer the difference beam pattern, the following phase distribution should be applied to the array elements [31].

$$\phi_k = \phi_o + (k-1)\Delta\phi + h_k \qquad (9.4\text{-}3)$$

where ϕ_o is an arbitrary phase reference common to all elements, and $\Delta\phi$ is the necessary phase shift that must be imposed to steer the main (difference) beam of the array at an angle $\theta_o = kd \sin \Delta\phi$. The additional phase h_k should be applied only to half of the array elements

$$h_k = \begin{cases} \pi\ , & k > N/2 \\ 0\ , & k < N/2 \end{cases} \qquad (9.4\text{-}4)$$

Assuming a linear coupled-oscillator array with adjacent element coupling, this is easily achieved by using an inter-element coupling network with coupling phase 0 deg between all elements except for the center elements where the coupling network phase is 180 deg.

More importantly, it was further shown by Heath [31] that the difference pattern can be scanned by simply detuning the free-running frequencies of the edge array elements, in the same manner that the sum pattern is scanned (Fig. 9-6).

In Ref. [151], Georgiadis and Collado applied the pattern synthesis optimization algorithm described in this section in a seven-element linear array, in order to synthesize a dual-beam pattern with beam directions at 15 deg and

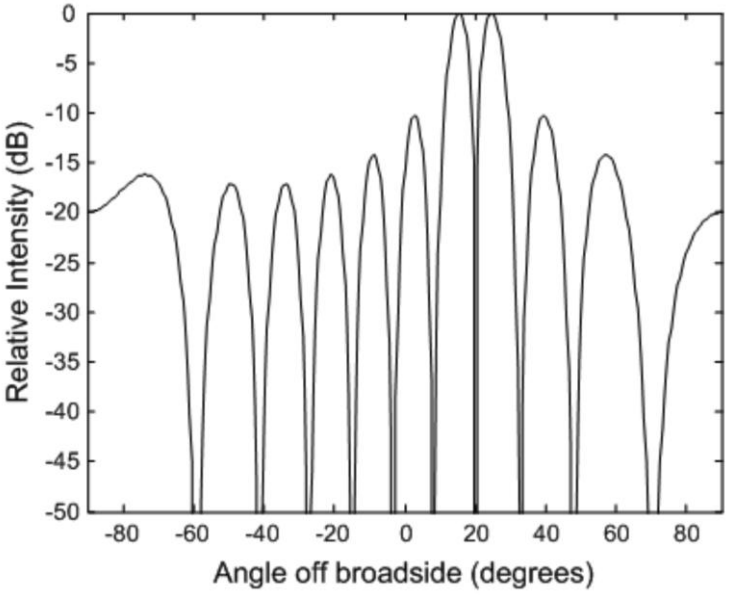

Fig. 9-6. Difference-pattern demonstration using a $N = 20$ element coupled oscillator array. The beam is steered at $\theta_o = 20$ deg according to Eq. (9.4-3). (Reprinted with permission from [31], ©2001 IEEE.)

-25 deg from broadside, while imposing a maximum level constraint of -20 decibels relative to the carrier (dBc) between the two beams. The array factor is minimized in the remaining angular directions, imposing the first constraint given by Eq. (9.4-2). The resulting necessary complex element excitations are shown in Fig. 9-7.

The desired phase differences are imposed on the coupled-oscillator array by allowing the free-running frequencies of all oscillators to be tuned. Amplitude control however, is imposed externally to the oscillator elements by employing variable attenuators (or variable gain amplifiers) at the oscillator outputs. The required excitations are introduced in a harmonic-balance simulator as follows. An ideal probe is connected to the output of each oscillator element, and the phase information is imposed in the probes. Harmonic balance optimization is then used to find the steady-state oscillator amplitudes and control voltages that correspond to the imposed phase distribution. Once the steady state is found, the oscillator output amplitudes are adjusted using attenuators so that the desired amplitude distribution is obtained.

It should be noted that after examination of the required excitation phases obtained from the optimization algorithm (Fig. 9-7), a coupling network was designed such that the coupling phase between elements 2 and 3, and 5 and 6, is 180 deg while the coupling phase of the remaining elements is 0 deg. The rationale behind this choice was that when the coupling network phase is 360 deg, a stable solution with phase difference in the range [–90 deg, +90 deg]

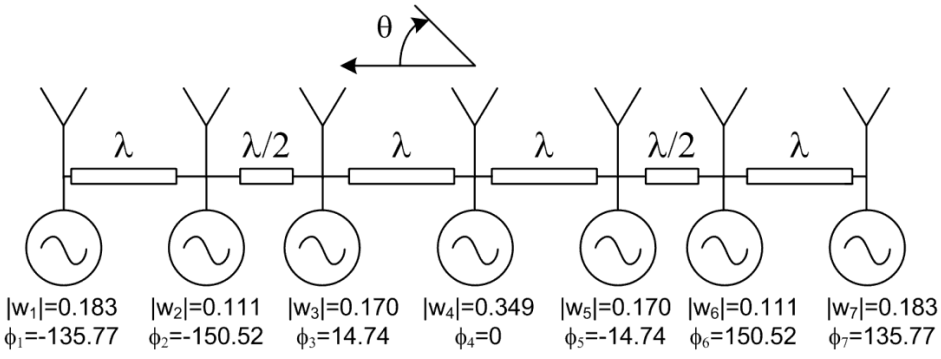

Fig. 9-7. Multi-beam pattern generation using a seven-element coupled oscillator array. Element excitations required to synthesize two main beams at 15 and -25 deg from broadside, with a maximum level constraint of –20 dBc between the two beams. The required coupling network phase shift to ensure a stable solution is indicated. Taken from [151]; copyright EurAAP 2009; used with permission.

can be obtained, whereas if the coupling phase is 180 deg, the stable solutions can have a phase difference in the range of [+90 deg, +270 deg]. As the required phase difference among elements 2 and 3, and 5 and 6, is more than 90 deg (see Fig. 9-7), a coupling network with phase of 180 deg was selected in order to ensure the existence of a stable solution.

The array factor corresponding to the excitations resulting from the solution of the optimization problem given by Eq. (9.4-2) is shown in Fig. 9-8, where it is marked as the ideal pattern. The coupled-oscillator array amplitudes found after the application of the above solution in a harmonic-balance simulator, as described in the previous paragraphs, were used to compute the coupled-oscillator array radiation pattern. The resulting pattern shows an excellent agreement with the ideal pattern. Finally, the array factor corresponding to uniform amplitude excitation and application of only the phase excitation values from Eq. (9.4-2) is superimposed in Fig. 9-8, showing that by imposing the phase condition only it is possible to successfully obtain the two desired main lobes, but it is not sufficient to maintain the sidelobe levels at a sufficiently low value.

Furthermore, it was verified that the two beam patterns can be scanned while maintaining their angular distance of 40 deg by detuning only the free-running frequencies of the end elements. The result of the harmonic-balance simulation is shown in Fig. 9-9. This last example may be viewed as a generalization of the difference pattern synthesis work of Heath [31], in the sense that once a desired phase and amplitude distribution among the array elements is obtained, thus synthesizing a desired array factor, a progressive constant-phase shift distribution may be superimposed by detuning only the end array elements, thereby permitting one to scan the synthesized pattern accordingly.

9.5 Control of the Amplitude Dynamics

Oscillator amplitude control provides an additional degree of freedom in order to synthesize more complex radiation patterns with improved performance capabilities, such as reduced sidelobes. The possibility of controlling the oscillator free-running amplitudes in order to synthesize a desired pattern was investigated by Heath [159]. Furthermore, in the works of Georgiadis et al. [118,150,153] the oscillator amplitude dynamics are included in the beamforming problem formulation. Recently, control of the amplitude dynamics of the coupled oscillator array, was also addressed by Jiang et al. [160], where the generation of triangular amplitude distributions in linear coupled oscillator arrays was demonstrated.

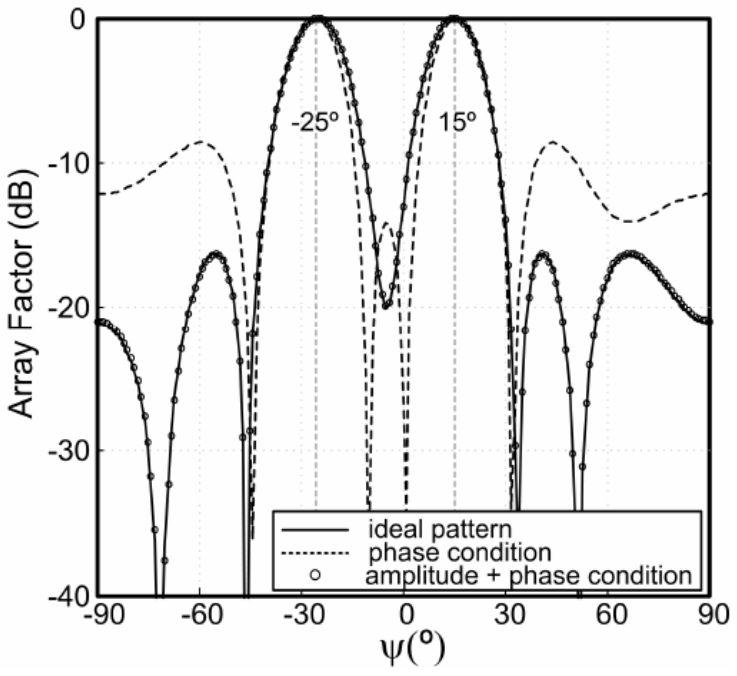

Fig. 9-8. Dual beam pattern generation using an $N = 7$ element coupled-oscillator array. The solution of the optimization problem (ideal pattern) is compared with the final solution for the array using harmonic-balance optimization (amplitude and phase condition) and with a pattern obtained imposing the phase excitation and uniform magnitude excitation (phase condition). Taken from [151]; copyright EurAAP 2009; used with permission.

Using a complex notation, the oscillator dynamics are described using either of the two models presented in Sections 7.4 and 7.6. The formulation of Heath [159] using the model of Section 7.4, is presented here

$$\dot{a}_m = j\Delta\omega_m a_m + \mu(A_{om}^2 - |a_m|^2)a_m + \sum_{i=1}^{N} \kappa_{mi} a_i \qquad (9.5\text{-}1)$$

with $a_m = A_m e^{j\phi_m}$. The periodic steady-state solution is obtained by setting $\dot{A}_m = 0$ and $\dot{\phi}_m = c$ with c an arbitrary constant, resulting in

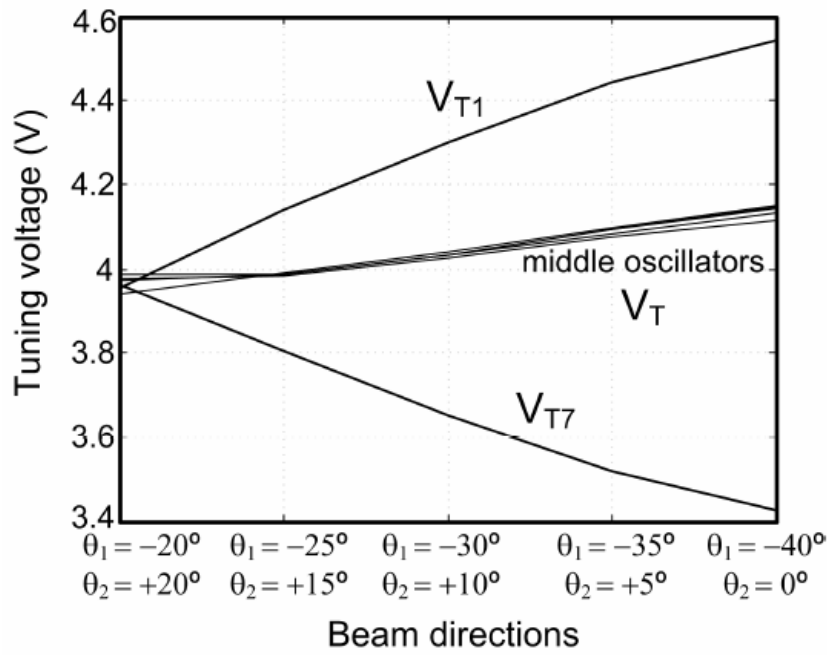

Fig. 9-9. Dual beam pattern steering using an $N = 7$ element coupled-oscillator array. Oscillator control voltages for different scanning angles. Taken from [151]; copyright EurAAP 2009; used with permission.

$$\rho_m = p_m + j\Delta\omega_m = jc + \mu|a_m|^2 - \sum_{i=1}^{N} \kappa_{mi} \frac{a_i}{a_m} \qquad (9.5\text{-}2)$$

with $p_m = \mu A_{om}^2$. Parameters p_m and $\Delta\omega_m$ allow one to independently tune the free-running frequency and free-running amplitude of the oscillator elements in order to synthesize a desired pattern. In Ref. [159], near-neighbor coupling was considered simplifying the coupling network matrix κ. Once a desired amplitude and phase distribution a_m is selected, one may separate the above equation into real and imaginary parts and solve for the tuning parameters, p_m and $\Delta\omega_m$. Finally, the stability of the solution must be examined through the eigenvalues of the linear variational equation given by Eq. (9.5-1), as was described in Section 7.4.

9.6 Adaptive Coupled-Oscillator Array Beamformer

In addition to the beamforming capabilities of coupled-oscillator arrays, an adaptive receive beamformer based on a coupled oscillator array was demonstrated by Ikuma et al. [154]. The steady-state expression of the coupled-oscillator array provides a means for controlling the array-element amplitudes

and phases by adjusting the free-running oscillator frequencies and the coupling network. Similarly to the previous paragraph, a complex notation for the array dynamics pertaining to either of the two models of Sections 7.4 and 7.6 may be utilized.

The formulation of Section 7.4, also shown in Eq. (9.5-1), was followed in Ref. [154]. The periodic steady-state solution is obtained by setting $\dot{A}_m = 0$ and $\dot{\phi}_m = c$ with c an arbitrary constant, resulting in

$$\rho_m a_m + \sum_{i=1}^{N} \kappa_{mi} a_i = b_m \tag{9.6-1}$$

where $m = 1,2 \ldots N$

$$\begin{aligned} \rho_m &= \mu A_{om}^2 + j\Delta\omega_m \\ b_m &= (\mu |a_m|^2 + jc) a_m \end{aligned} \tag{9.6-2}$$

Finally, in matrix form one has

$$(\boldsymbol{\rho} + \boldsymbol{\kappa})\boldsymbol{a} = \boldsymbol{b}(\boldsymbol{a}) \tag{9.6-3}$$

where $\boldsymbol{\rho}$ is a diagonal matrix with ρ_m in its main diagonal and $\boldsymbol{b}$ is a vector with b_m in its main diagonal. Matrix $\boldsymbol{\rho}$ contains the oscillator parameters, the free-running amplitudes, and the free-running frequency offsets from ω_o. The frequency offsets can be adjusted, whereas the free-running amplitudes are fixed and assumed equal for all oscillators. Amplitude control may also be achieved using, for example, a variable attenuator or variable-gain amplifier at each oscillator output. The matrix κ contains the coupling-network gain and phase, and it may also be tunable. In Ref. [154], nearest neighbor coupling is assumed, which results in a bi-diagonal matrix $\boldsymbol{\kappa}$.

There are many possible combinations of $\boldsymbol{\rho}$ and $\boldsymbol{\kappa}$ that can lead to a desired complex amplitude vector $\boldsymbol{a}$. Ikuma et al. [154] considered a reconfigurable coupling network $\boldsymbol{\kappa}$ and identical oscillators without frequency tuning, leading to a fixed $\boldsymbol{\rho}$ matrix. As a result, the coupling matrix $\boldsymbol{\kappa}$ is used to generate the desired amplitude distributions a.

The proposed adaptive receiver of Ikuma et al. [154] is shown in Fig. 9-10. Assuming a receiving uniform linear-antenna array of N elements, the received signal vector from all antennas is $\boldsymbol{r}(t)$.

The received signal is split into two signal paths. The signal in the first path is mixed with a reference oscillator $z_r(t)$, and after passing through a low-pass filter to remove unwanted mixing products, it provides the reference vector

$\boldsymbol{r_a}(t)$. In the second path, the received signal vector is mixed with the coupled-oscillator array vector $\boldsymbol{z}(t)$; and after low-pass filtering, it provides the demodulated scalar output signal $y_a(t)$ of the beamformer. The fixed oscillator is phase locked to the middle element of the coupled-oscillator array. It should be noted that in the block diagram of Fig. 9-10, the analytic representation [149] of the various signals is indicated. As an example, the analytic signal of the reference oscillator is

$$z_r(t) = w_r e^{j\omega_o t} \tag{9.6-4}$$

with ω_o the reference oscillator frequency and w_r its complex amplitude.

The coupled-oscillator array complex amplitudes are adaptively controlled based on a least-mean-square (LMS) algorithm given by

$$\dot{\boldsymbol{a}} = -\mu \boldsymbol{M} \boldsymbol{r_a}(t) y_a{}^*(t) \tag{9.6-5}$$

in order to minimize the effect of unwanted interfering signals present in the received array signal $\boldsymbol{r}(t)$. The operator ()* denotes the complex conjugate. Matrix $\boldsymbol{M}$ depends on the desired fixed constraints of the beamformer, in other words, on a set of specified array-factor levels at a number of angular directions

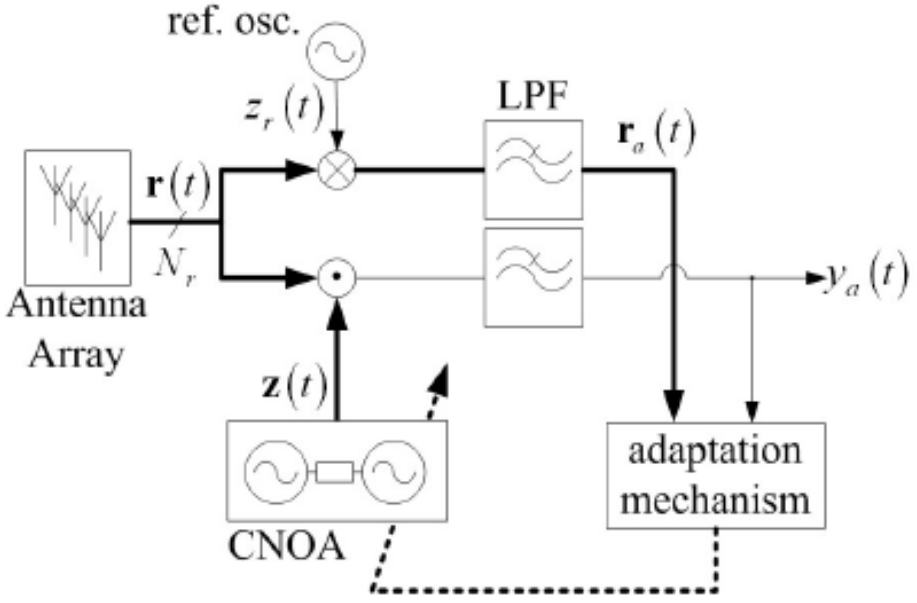

Fig. 9-10. Adaptive coupled-oscillator array receiver block diagram. (Reprinted with permission from Ref. [154**], ©2001 IEEE.)**

including the direction of arrival of the main beam [154]. Finally, the parameter μ controls the convergence speed of the beamformer. The proposed beamformer operation was verified by computer simulation.

9.7 Conclusion

In this chapter we introduced several optimization problems, demonstrating the beamforming capabilities of coupled oscillator arrays. The beamforming problem has been formulated as a convex optimization problem, which includes the array steady state as a linear constraint. The results of Chapter 7 have been used to provide an expression for the steady state of the coupled-oscillator array. Additionally, the capability of generating and scanning multiple beams has been verified. Furthermore, a non-convex optimization algorithm, which optimizes the stability of the steady state solution, has been introduced, and an adaptive beamformer based on coupled oscillator arrays has been demonstrated. The combination of optimization and signal-processing techniques (together with the rich dynamical properties of coupled-oscillator arrays) reveal the potential and numerous applications of such arrays, which have yet to be explored.